PHYSICS

Some Measurements on the Vapor Viscosities of the Two Common Pentanes, Two Pentenes, and Carbon Tetrachloride

By WILLIAM M. BLEAKNEY
California Institute of Technology

(Received July 5, 1932)

The present work is a continuation of the investigations begun by Dr. R. K. Day on the behavior of vapors by means of accurate viscosity measurements. The instrument, designed and built by him, has been improved, and his results on normal and iso-pentane have been verified.-In addition, measurements on two pentenes, similar in structure to the pentanes, have been made at room temperature, and the viscosity-pressure curves for all four hydrocarbons and also for CCl_4 have been obtained at 100°C. A linear relation, with a negative slope, persists in all these curves, the slope for the hydrocarbons being considerably less at the higher temperature, while the curve for CCl_4 is comparable to those for the hydrocarbons at room temperature. Following are the values of the constants in the equation $\eta = \eta_0(1 - \alpha p)$, the pressure being expressed in atmospheres.

Vapor	25°		100°C	
	$\eta_0 \times 10^6$	100α	$\eta_0 \times 10^6$	100α
normal pentane	67.593	1.15	84.070	0.41
2-pentene	68.927	1.09	85.820	0.24
iso-pentane	69.529	1.04	85.951	0.33
trimethylethylene	70.051	1.30	86.852	0.32
CCl_4			121.78	1.08

INTRODUCTION

THE present work of studying the behavior of vapors near saturation by means of viscosity measurements was begun by Dr. R. K. Day under the direction of Dr. R. A. Millikan, and the first results, some measurements on normal and iso-pentane, are discussed by him in a previous paper.[1] The negative slopes of the viscosity-pressure curves found by him were entirely new in gas viscosity measurements, the common gases having always a positive slope. Since, however, the work represents the first application of a new and elaborate viscometer built by him, difficulties were encountered in making the measurements, and it was not certain that the data were sufficiently accurate to draw definite conclusions.

Accordingly work was begun to improve the instrument, the intention being to repeat measurements on the pentanes at 25°C in order to establish their accuracy. In the meantime, carefully prepared samples of the two

[1] R. K. Day, Phys. Rev. **40**, 281 (1932).

pentenes, whose structure is most nearly like the pentanes, were received from the Standard Oil Development Company of Elizabeth, New Jersey, along with samples of normal and iso-pentane which had been obtained from natural sources. Since the pentane samples at hand were synthetic, it was thought worthwhile to compare viscosity values obtained from the new samples with the old values, as a check upon the purity of the materials. Also measurements were made on the pentenes, in the belief that a knowledge of the effect upon viscosity of the removal of two hydrogen atoms from the pentane molecule and the substitution of a double bond would be of value.

Later, when measurements at higher temperatures were made possible, observations were taken on carbon tetrachloride, thus making possible a comparison of a molecule of simple structure with the more complicated hydrocarbons, both being in the vapor state.

Attempts have been made, but without success, to obtain the third isomeric pentane, a molecule of which is symmetrical, according to the chemists' structural formula, about a central carbon atom. It is of special interest to observe the difference in the viscosity of isomers, because this gives directly the effect of molecular structure upon the mean free path.

Instrumental Changes

The method of measurement used is the rotating cylinder method, chiefly because it is capable of high precision and is also applicable at low pressures. The instrument is described in detail in Dr. Day's paper and only the more important changes which have been introduced since his work will be given here.

Early difficulties in keeping the instrument casing vacuum tight were thought to be due largely to the lightness of some of the metal parts, the strains set up by frequent evacuation being sufficient to form cracks in the large solder joints. Accordingly, some of the lower parts were made stronger and all the joints carefully resoldered. This did not eliminate the difficulties, however, and only by carrying out an extended program of locating and stopping the leaks as they formed during the progress of the work has it been possible to attain good working conditions.

The vapors to be examined have a strong solvent action upon nearly all organic materials, so it was advisable to prevent contact of the vapors with any waxes, cements, rubber, or grease. All gaskets are made of lead, the joints are either solder or copper-glass seals, and the stop-cocks are all metal, consisting of a needle valve operated by means of a sylphon. The window is a quarter inch glass plate strongly clamped to the plane brass window face, with a fine lead fuse wire soldered at the ends to form a loop for a gasket.

During the early work it seems that some organic material got deposited within the instrument which gave trouble when the vapors reached pressure near saturation, and repeated efforts to clean the parts separately were unsuccessful because of their complicated structure, nor could the deposit be pumped out. Finally the entire instrument was filled with liquid carbon tetrachloride, which was warmed and circulated several days, then drained as

far as possible and pumped out. This removed the foreign material but rusting of the steel parts set in afterward, probably started or hastened by impurities in the carbon tetrachloride. Finally it became necessary to replace the suspension and one of the ball bearings upon which the outer cylinder turns. The upper steel parts were copper plated to prevent further rusting.

The new suspension is somewhat stronger than the old one, having a cross section of about 2.2×5.8 mils, so that the period of the inner cylinder is now 150 seconds instead of 198. The steel ribbon was first heated to about 400°C for several days while supporting a light weight in order to form a protective layer of oxide to resist the rust action. It was then carefully annealed while supporting a load of 900 g by gradual cooling over a period of two days. When mounted, the new suspension showed a remarkably constant zero position and a much smaller drift while in the deflected position, this drift being of the order of 0.005 percent per minute as compared to 0.04 percent for the old one. As will be seen, the drift becomes considerably larger, however, at higher temperatures.

In order to compensate for the loss in sensitivity caused by the larger torque constant, the scale has been moved back to a distance of 478 cm from the mirror, and the telescope mounted near the window, thus doubling the sensitivity of the optical system without affecting the magnification or resolving power. A possible error in the early measurements may be due to pendular oscillations of the inner cylinder, and the long mirror-to-scale distance has the added advantage of making these oscillations more easily observed. With this system deflections can be read with an accuracy of about 0.02 percent.

During the progress of the work it has been necessary completely to dismantle the instrument several times, and in reassembling the method of aligning the cylinders is of course important. The beam supporting the inner cylinder is first adjusted so that the outer surface of the cylinder is strictly vertical. This can be done by means of plumb bobs and a cathetometer within 0.05 mm. The cylinder is then hung in the instrument and the guard cylinders brought in line with the suspended cylinder by adjustment of the suspension head and the base supports. The two main cylinders will then be coaxial if the machining of the bearings and supports is accurate.

In the past, a slight settling of the base supports on one end of the pier has been observed, which will throw the cylinders slightly out of line, but since the speed of rotation is so adjusted that the deflections are all of the same order of magnitude, the mean distance between the cylinders across which the viscous action takes place will not change between successive runs. This is especially true if the inner cylinder rotates upon its own axis, a condition which depends only upon the initial adjustment, so that in relative measurements no error is expected from this quarter.

The Bourdon spiral pressure gauge of Pyrex tubing has been improved to obtain greater sensitivity and to make it applicable for measurements at higher temperatures. A stellite mirror is soldered to a needle, the ends of which are ground to fine points, and mounted in small glass sockets. A short

copper wire, also soldered to the back of the mirror, makes possible the adjustment of the system so that it is very nearly balanced. The mirror is thus held in contact with the extended arm of the spiral only by gravity and, there being no elastic properties involved except those of the spiral itself, the deformation of which is exceedingly small, neither the zero position nor the calibration constant is appreciably affected by a change of temperature. The sensitivity obtained is about 16 mm deflection for a change of pressure of 1 mm of mercury. The chief inaccuracy is in the reproducibility of the zero reading due to the considerable play which the needle points have in the glass sockets. Except at low pressures, the gauge is used only as a null instrument, the pressure being read on a manometer which is connected to the opposite side of the spiral from the instrument.

In order to prevent any stresses being set up between the evacuating system and the top of the instrument which may throw the cylinders out of alignment, the inlet tube is a long copper tube with a deep "goose-neck" near the instrument.

Neither the constant speed motor described by Day nor the rotating field device used for controlling the oscillations of the inner cylinder has required modification.

Measurements at Room Temperature

It, of course, is essential in all measurements that no tendency toward turbulent flow be present. The threshold of turbulence is expected to depend upon the ratio $\rho vl/\eta$ where ρ is the density, v the velocity of the outer cylinder, l the distance between cylinders, and η the viscosity. A test was carried out under the most extreme conditions of this ratio available, namely isopentane at saturation pressure with the speed of the cylinder at two revolutions per minute, but no tendency toward turbulence could be observed.

This is sufficient justification for the procedure of adjusting the speed of the cylinder so that the deflections in all measurements are about the same. Thus for air a gear ratio at the motor of 9:14 is used, while for the hydrocarbons a ratio of 14:9 is applied. Such a procedure tends to minimize errors which may occur from several sources, such as poor alignment of the cylinders, suspension drift, the conversion of straight scale readings to angles, and inaccuracies in the scale itself.

The motor being reversible no zero reading is used, the sum of the deflections taken each way from the zero being all that is desired. The telescope is adjusted so that the zero reading falls very near to the center of the scale, which is the foot of a perpendicular drawn from the mirror to the scale, so that the two deflections are always very nearly equal. Because of the slight suspension drift, a definite time schedule is followed in taking readings, the mean value obtained five minutes after the cylinder crosses its zero position being used in all cases so that no correction for drift is necessary. This gives sufficient time for any transient effects arising during the reversal of the motor to die out, and also permits sufficient readings on the turning points to obtain a good average.

It is well known that at low pressures slippage occurs between the gas and the walls which is important only when the mean free path is not a negligible fraction of the distance between the walls. Assuming no specular reflection of the molecules at the walls, Millikan[2] finds for the slip factor $1+0.7k\lambda$ where λ is the mean free path and the instrument constant, k is given by

$$k = 2(a^3 + b^3)/(ab^3 - a^3b)$$

a and b being the radii of the cylinders. The correction is inversely proportional to the pressure and amounts to the following values at 1 mm pressure

Substance	at 25°C	at 100°C
air	1.65%	2.19%
pentane	0.38%	0.55%
CCl_4		0.52%

Measurements taken on air at low pressures were found to be in complete agreement with the above equation. The correction has therefore been applied to all measurements where the correction is appreciable in order to obtain the true viscosity.

TABLE I. *Sample of data. Normal pentane; gear ratio = 14:9; pressure = 2.0 cm.*

Direction of motor	Time	Turning points	Equilibrium position		Deflection
East	11:37:00 A.M.				
24.98°C	38:30	25.44 cm			
	39:45	24.96	25.195 cm		
	41:00	25.42	.190		
	42:15	24.96			
West	11:43:30				
	44:30	74.86			
	45:45	75.49	75.185		
	47:00	74.89	.188		
	48:15	75.48	.190		75.190 cm
	49:30	74.91			25.188
East	11:50:45				50.002
	52:00	25.15			
	53:15	25.24	25.195	slip	
	54:30	25.15	.192		.010
25.00°C	55:45	25.25	.188		50.012
	57:00	25.14		temp.	
Stopped		Zero position 50.189 cm			.001
					50.013

The time given when the motor is reversed is the time at which the cylinder crosses its zero position.

The values obtained in the last column under "deflection" are plotted against the pressure to obtain the curves shown. (See Fig. 1.) The values obtained at the ends of the curves are then converted to arc lengths, which changes them very little. To the zero pressure intercept is added a very small term to account for the refractivity of the air outside the window, and the

[2] R. A. Millikan, Phys. Rev. **21**, 231 (1923).

result compared with the deflection obtained for air, also reduced to arc lengths, to obtain the true limiting value of the viscosity η_0.

To obtain the pressure variation, that is, the value of α in the equation $\eta=\eta_0(1-\alpha p)$ the negative slope of the curve expressed in percent per atmosphere is added to the refractivity of the vapor expressed in the same units. This last correction is important and constitutes almost the only difference between the present values of α and those of Day, who neglected to consider the refractivity. The values used are obtained by plotting the apparent zero position of the cylinder against the pressure. The zero position is obtained by averaging the values given in the column headed by "equilibrium position" instead of taking their differences, as was done to get the deflection. Since the telescope is mounted a little to one side, making an angle of about 13.5° with the normal to the window, the variation of the apparent zero position with pressure is appreciable, being about 2 mm, and from the slope of this curve and a knowledge of the angles involved the refractivity may easily be computed with an accuracy sufficient for our purpose. The values obtained agree satisfactorily with the one rather doubtful value given in the International Critical Tables for pentane.

The values used (in percent per atmosphere) for 25°C are:

normal pentane	0.157%	trimethylethylene	0.155
iso-pentane	0.157	carbon tetrachloride	0.130 (at 100°)
2-pentene	0.155	air	0.027

At other temperatures the values may easily be computed since they are inversely proportional to the absolute temperature.

The calibration constant of the instrument is simply obtained by using the known value[1] of the viscosity of air at 25°C, namely 183.25×10^{-6}. The deflections obtained for air are very consistent provided due precaution is taken to remove traces of the vapors which may adhere to the walls of the instrument for some time. For example, the values obtained before and after the four runs at room temperature here given differed by only 0.006 percent. A very slow decrease in these values with time has been observed, amounting to about 0.1 percent in five months and is believed to be due to actual stiffening of the suspension caused by the considerable tension on it, an effect which has been observed by other investigators in similar suspensions.

An estimate of the probable errors in the values of α can best be obtained from an examination of the curves given, but an estimate of the accuracy of the absolute values of the viscosity is much more difficult to make, as will be seen from the following discussion.

The first measurements on a vapor at low pressures are almost invariably too high, sometimes as much as one percent higher than the final values. After repeated flushing out of the instrument at a few centimeters pressure, the points are found to lie fairly close to the final curve, but it is only after higher pressures have once been reached that really consistent results are obtained. These initial discrepancies are almost certainly due to impurities, principally air, and various methods of treating the vapors before admitting

them to the instrument have been tried, but without seeming to have much effect. It is believed that the heavy vapors displace the light gases from the walls and the gases, after being thoroughly mixed with the vapors at the higher pressures, represent only a small percentage of impurity and the composition of the vapors will thereafter remain unchanged during the course of the observations.

The initial points are not plotted on the curves, but after consistency has once been established, no observations are discarded and the pressure range is always covered several times. The fact that no difference is observed between points obtained while going up the pressure range from those obtained during the reverse process is strong evidence in support of the above view.

Runs have been taken on both the synthetic and the natural samples of iso-pentane and satisfactory agreement was obtained. The present data on both pentanes were taken from the original synthetic samples upon which Day made his measurements but these values for η_0 are about 0.2 percent lower than his. This difference may be due to less efficient methods of removing the air from the vapors in the earlier work, since P_2O_5 was used for a drying agent, from which it is very difficult to remove the air.

The two high points on the iso-pentane curve near saturation are believed to be due to condensation of liquid on the cylinders caused by an attempt to force the pressure too high. The discrepancy disappeared after the vapor was held for some time at a pressure slightly below saturation. The ends of the curves represent in all four cases complete saturation.

The Temperature Control System

The importance of the temperature control system in these experiments can not be over-emphasized. This will be realized more clearly when one remembers that the normal speed of the rotating cylinder is about 6 mm per second so that a convection current in the neighborhood of the inner cylinder having a speed of only a half a millimeter per minute may cause an appreciable disturbance, and since the vapors are adsorbed to a very large extent on the walls, a slight local change in temperature may cause large convection currents.

During the measurements at room temperature, (see Fig. 1), the temperature of the entire room was controlled so that the temperature of the instrument seldom varied by more than a tenth degree from the desired value of 25°C. For work at higher temperatures, the instrument is enclosed in felt one inch thick, with only the magnetic clutch and the three legs protruding. The loss of heat from these parts is compensated by heating coils wound directly on them. This compensation need not be accurate because the parts are not directly connected to the cylinder chamber.

Other coils are wound at different heights about the cylinder casing with from one to two inches clearance between the casing and the bare wires. A tube extending nearly the full length of the enclosure and made of thin felt, provides a path for the circulating air, which is drawn up through the tube by means of the fan marked *J* in the drawing, (see Fig. 2), and driven down past the heating coils. The fan is driven by a motor from the outside.

A massive copper block *H* contains two holes bored nearly to the bottom, in one of which is placed a Beckman thermometer which can be read from the outside. In the other are mounted the junctions of several copper-constantan thermocouples, their opposites being mounted in small copper tubes soldered to various parts of the instrument. There are two near the top of the

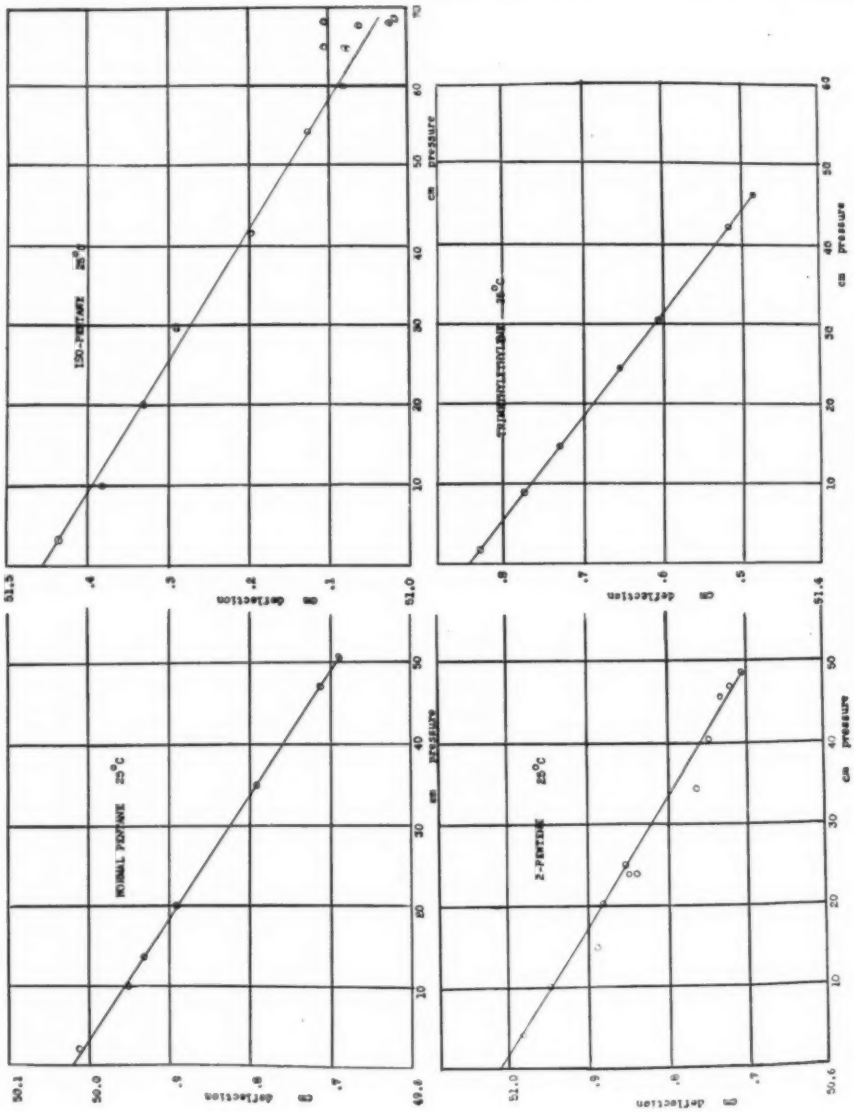

Fig. 1. Measurements at room temperature.

cylinder casing, two near the bottom, one on the base plate which is supported directly by the legs, one on one of the legs, and one on the magnetic clutch housing. The thermocouples may be connected by means of switches to a galvanometer on the outside, which has a sensitivity of about 10 cm per 0.1° difference in the temperature of the junctions. The copper block has a

tendency to remain slightly below the mean temperature of the instrument, so that a small current in a heating coil wound on it is sufficient to keep these temperatures very nearly the same. The currents are adjusted in the main heating coils until there is no appreciable temperature gradient along the cylinder casing as shown by galvanometer deflections. These four thermocouples are then connected in series to give, together with the thermometer readings, the temperature of the main part of the instrument.

When this adjustment has been made, the expansion tubes *K* provide an automatic control. These are filled with xylol in contact with mercury at the top which closes a relay circuit by making contact with a needle adjusted at the proper height in the small upper tube. The relays increase or decrease the current in the heating coils by only a small amount. This arrangement does not permit the temperature to vary by more than 0.1° during a run provided the outer magnets on the magnetic clutch are kept going, while this variation can be measured to 0.01°.

A double mica window permits observations on the inner mirror through the felt wall.

The Vapor Purification System

The vapor to be studied is first frozen down and sealed on at *A* and the entire system evacuated. (See Fig. 2.) Cock No. 1 is then closed and the material distilled over into the fractionating column *B* where it is fractionated,

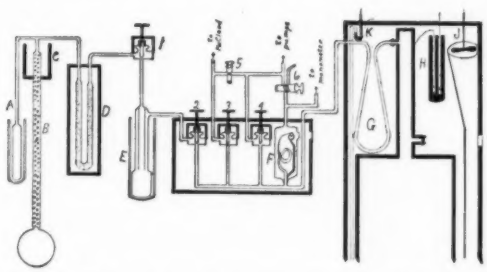

Fig. 2. The gas and temperature control system.

using ice in the reflux chamber *C*, the first components being drawn off occasionally through the cock and removed by the pumps. The principal purpose of the column is to separate the air, but it, of course, will also help to separate any other impurities including water. It is a recent addition and has been used only in the case of carbon tetrachloride.

The trap *E* is then immersed in liquid air and a slow stream of vapor permitted to pass through the drying tubes and freeze out in *E* at very low pressures. The drying tubes are filled with $Mg(ClO_4)_2 \cdot 3H_2O$ which is supposed to be nearly as efficient as P_2O_5 and has the advantage of never losing its crystalline form since it takes up the water to form the hexahydrate. It can be renewed simply by heating in vacuum by means of the furnace *D*.

When sufficient material has collected, cocks 1, 2, 3, and 4 are closed and the trap allowed to warm up. The vapor is then admitted or withdrawn from the instrument at will through cock No. 2. Cock No. 3, leading to the Mc-

Cleod gauge, is not essential but provides a parallel path to the pumps through cock No. 5 which speeds up the pumping considerably since the metal cocks have only a small opening.

Since pressures in the instrument are sometimes required above the saturation pressure at room temperature, provision must be made to heat the system extending from cock No. 1 to the instrument. The connecting tubing has been wound with resistance wire, the trap can be put in hot water, and the other cocks and the spiral pressure gauge F are enclosed in a felt box which can be heated to any desired temperature. The pressure of air on the outside of the spiral is made nearly equal to the pressure in the instrument by means of cock No. 6.

The loop of copper tubing G, aside from its purpose of preventing lateral forces on the top of the instrument, also prevents any cool vapor from entering the instrument directly, which may cause internal temperature gradients. The fan, copper block, and felt housing are supported from the ceiling so that no excess weight will be acting on the pier.

Measurements at 100°C

The standard formula for the rotating cylinder apparatus[2] is:

$$\eta = \frac{\pi\theta I(b^2 - a^2)}{a^2b^2P^2l\Omega}$$

where θ is the angle of deflection; I, the moment of inertia of the suspended system; b and a, the radii of the outer and inner cylinders; P, the natural period of the suspended system; l, the length of the inner cylinder; and Ω, the angular velocity of the rotating cylinder. For a given gas, we may, therefore, write for any temperature t:

$$\eta_t = \eta_{25}\theta_t P_{25}^2(1 + a\cdot 25)/\theta_{25}P_t^2(1 + at)$$

where a is the linear coefficient of expansion of the cylinders, and the angular velocity is the same at the two temperatures.

The periods are measured in vacuum in order that the moment of inertia will not be affected by gas moving with the cylinder and to reduce the damping coefficient. The period is found to be independent of the amplitude within the accuracy of measurement, which indicates that the rate of drift is truly proportional to the deflection so that it will have no first order effect upon the period but only increases the damping coefficient. The effect of the damping coefficient upon the period is about 0.002 percent. Since the drift rates are not the same at the two temperatures, the deflections must be reduced to zero time interval by means of the known drift rates before applying this formula.

We obtain in the case of air, the following values: $L\theta_{25} = 55.933$ cm, $P_{25} = 150.574$ sec., $L\theta_{100} = 67.991$, $P_{100} = 152.487$, $a = 1.67 \times 10^{-5}$ per degree for bronze, L is the mirror-to-scale distance.

This gives for air

$\eta_{100} = 216.93 \times 10^{-6}$ poises $\qquad S = 112.3$

where the Sutherland constant S is obtained from the Sutherland formula:

$$\eta = AT^{3/2}/(S + T).$$

The above results are in good agreement with those obtained by capillary tube methods.

With this value of η_{100}, the vapor viscosities can be obtained in the same way as before by comparing the deflections with those for air after the same time interval. The interval used in these measurements is six minutes.

TABLE II. *Sample of data. Normal pentane; gear ratio = 14:9; pressure = 73.0 cm.*

Direction of motor	Time	Turning points	Equilibrium position	Position on 6th min.
West	11:17:30 A.M.			
100.03°C	19:45	81.47 cm		
	21:00	82.44	81.988 cm	
	22:15	81.60	82.010	
	23:30	82.40	82.038	82.04 cm
100.02°C	24:45	81.75		
East	11:26:00			
	29:00	18.34		
	30:15	17.93	18.122	
	31:30	18.29	.108	18.105
100.05°C	32:45	17.92	.102	
	34:00	18.28		
West	11:35:15			
	37:45	81.80		
	39:00	82.10	81.965	
	40:15	81.86	82.000	
100.04°C	41:30	82.18	82.032	82.03
	42:45	81.91		
East	11:43:45			
	46:45	18.40		
100.05°C	48:00	17.89	18.118	
	49:15	18.29	.082	18.07
	50:30	17.86	.060	
Stopped	51:45	18.23		

Deflection: 82.035 − 18.085 − 0.01 = 63.94

The data at 100° (see Fig. 3) are not quite so consistent as those taken at room temperature, partly because the drift rate is much larger and partly because the temperature variations are more rapid. The three high points on the CCl_4 curve (Fig. 4) were taken in succession at the end of the run and are not believed to be as reliable as the others because a slight leak was found in one of the stopcocks later.

The curves do not represent viscosity until after the correction for the refractivity of the vapor has been applied and this in some cases nearly doubles the magnitude of the slope.

NUMERICAL RESULTS

Representing the viscosity by means of the equation

$$\eta = \eta_0(1 - \alpha p)$$

where p is the pressure in atmospheres, and obtaining the values of these constants from the curves in the manner previously described, the results shown in Tables III and IV are obtained.

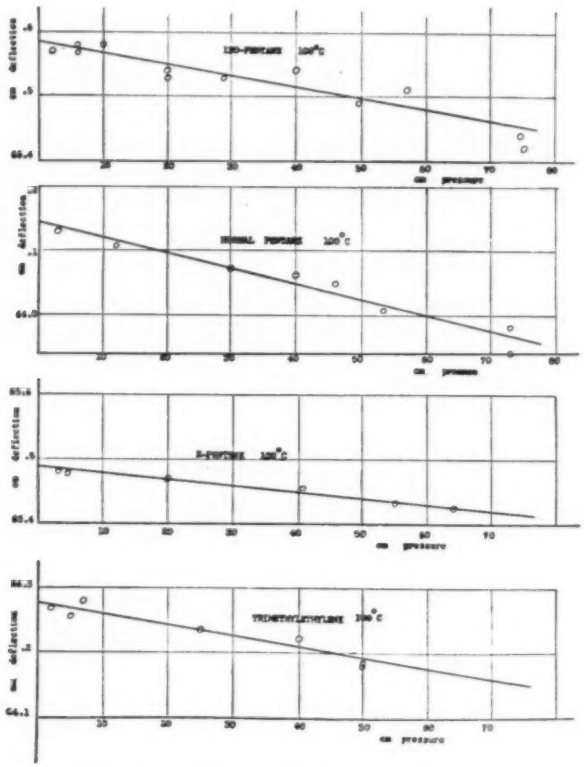

Fig. 3. Measurements on the hydrocarbons at 100°C.

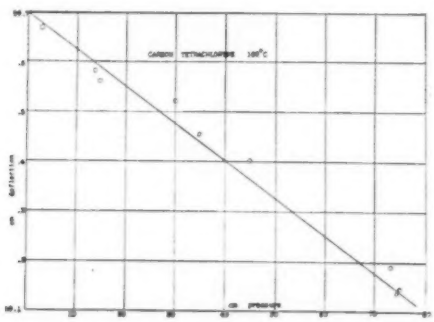

Fig. 4. Measurements on CCl_4 at 100°C.

It will perhaps be more instructive to refer the slope of the curves to molecular density instead of to the pressure, so that the values at different temperatures will be on a more comparative basis. If we write

$$\eta = \eta_0(1 - \alpha'\rho)$$

TABLE III. *Viscosities at 25°C.*

Substance	$\eta_0 \times 10^6$	100α	Structure
normal pentane	67.593	1.15	$CH_3-CH_2-CH_2-CH_2-CH_3$
2-pentene	68.927	1.09	$CH_3-CH=CH-CH_2-CH_3$
iso-pentane	69.529	1.04	$CH_3-CH_2-CH(CH_3)(CH_3)$
trimethylethylene	70.051	1.30	$CH_3-CH=C(CH_3)(CH_3)$
air	183.01	−0.13	

TABLE IV. *Viscosities at 100°C.*

Substance	$\eta_0 \times 10^6$	100α	S	*B.P.*
normal pentane	84.070	0.41	298.7	36°C
2-pentene	85.820	0.24	304.2	36.5
iso-pentane	85.951	0.33	267.5	27
trimethylethylene	86.852	0.32	282.7	38.4
carbon tetrachloride	121.78	1.08		76.7
air (atmospheric pressure)	216.93		112.3	

where ρ is the molecular density referred to the density of an ideal gas at 0°C and one atmosphere pressure, α' may be obtained from the above values by means of the relation

$$\alpha' = (\alpha T/273)(1 + B/V)$$

where B is the second virial coefficient and V is the volume at a pressure of one atmosphere.

TABLE V. *Values of $100\alpha'$.*

Substance	25°C	100°C
normal pentane	1.21	0.55
2-pentene	1.14	0.32
iso-pentane	1.09	0.44
trimethylethylene	1.36	0.43
carbon tetrachloride		1.42
air	−0.14	

It will be seen that, for both temperatures, the values of η_0 are in the order in which we might have predicted them, those hydrocarbons for which we should expect, from the structural formula, the least cross section, having the largest viscosity.

The values of Sutherland's constant S given in the second table are computed from the equation $\eta_0 = AT^{3/2}/(S+T)$ but this equation is not expected to hold at these low temperatures except in the case of air. This is borne out by the unusually low values given, S being for most substances slightly higher than the critical temperature, and the critical temperatures for normal and iso-pentane are 470° and 461°K respectively. In fact, Rappenecker,[3] from measurements on iso-pentane at 100°C and 212° C by the capillary tube

[3] Rappenecker, Zeits. f. phys. Chem. **72,** 695 (1910).

method, finds the value $S=500$. His value for η, 88.51×10^{-6} at 100°C and atmosphereic pressure, is 4 percent higher than mine, but he used for calibration purposes a value for air $1\frac{1}{2}$ percent higher than mine, and the remaining difference of $2\frac{1}{2}$ percent is not surprising in view of the rather doubtful reliability of the capillary tube method when applied to highly adsorbing vapors. No other values are listed for these materials.

The most important contribution, however, of the present investigation is the establishment of the negative slopes of the viscosity pressure curves, a condition which persists at temperatures much higher than the boiling point, whereas, all previous measurements, save those of Day, have been made on gases and show a positive slope. The present measurements suggest that probably all vapors act in the same way at sufficiently low temperatures, and one can not help but remark upon the parallel behavior of the second virial coefficient as related to pressure. The hypothesis has been advanced[4,5] that $(-\alpha)$ is very closely connected with, perhaps equal to, van der Waal's coefficient b, but it seems to behave more like the virial coefficient of which b is only a part. The two must however, be explained on different grounds. It is desirable that the present viscosity theory be analyzed more carefully and extended to obtain the first order pressure effect. It is suggested that triple collisions may play an important role, and that molecular association may be present at these low temperatures, undetected by compressibility measurements alone. An attempt to treat the theoretical problem is now in progress. It is hoped that these investigations will throw more light upon the process of condensation. In this connection it is of interest to note that no departure from linearity is observed near saturation in any of the curves.

One would like to extend these observations to obtain the temperature dependence of α more closely and over a wider range, as well as of η_0, and perhaps to go to higher pressures but with the instrument in its present condition, it is not considered safe to go much above atmospheric pressure, and the upper limit of temperature is probably about 150°C where the accuracy will be much reduced because of the increased suspension drift. Some knowledge of the effect of temperature on α may be obtained, however, by examining other materials representing different stages of the transition from a gas to a vapor, and such observations would of course, be valuable for other purposes.

Credit for the success of the work is largely due to Dr. R. A. Millikan, under whose supervision it has been carried out, and to Dr. R. K. Day and Mr. Julius Pearson for the excellence of the design and construction of the instrument.

[4] H. B. Phillips, J. Math. and Phys. (M.I.T.) **1**, 42 (1921).
[5] J. H. Boyd, Phys. Rev. **35**, 1284 (1930).

The Crystal Structure of Black Nickel

By H. KERSTEN AND JOSEPH MAAS
Department of Physics, University of Cincinnati

(Received July 6, 1932)

This paper shows by means of x-ray diffraction analysis that electrodeposited black nickel has an amorphous structure which changes to a crystalline structure when the deposit is heated.

INTRODUCTION

BLACK nickel is an electrodeposited mixture of nickel, sulphur, zinc, and in some cases organic material. It appears probable that the nickel and sulphur are combined in the form of nickel sulphide.[1] It is used on hardware, military equipment, and wherever a black metallic coating is desired.

EXPERIMENTAL

The plating bath used[2] had the following composition: water, 1 liter; nickel ammonium sulphate, $NiSO_4(NH_4)_2SO_4{:}6H_2O$, 50 g; ammonium thiocyanate, NH_4SCN, 10 g; zinc sulphate, $ZnSO_4{:}7H_2O$, 6 g. Stainless steel cathodes to which the deposits did not adhere well and from which they could easily be stripped, and rolled nickel anodes, were used. The hydrogen ion concentration of the bath, measured with a quinhydrone electrode was 5.4, the current density, 0.5 amp./dm^2, and the temperature of the bath, 30°C. The x-rays were supplied by a gas tube having a nickel target, operated at 30 m.a. and 25 k.v., equipped with a reflection spectrograph. The tube and spectrograph have been described elsewhere.[3] [4]

RESULTS

Fig. 1 shows the diffraction photograph of a sample of black nickel which had been deposited on stainless steel, cracked off by bending the steel, and ground to a powder in an agate mortar. Exactly the same kind of picture was

Fig. 1. Diffraction photograph of amorphous black nickel.

obtained when the sample was not removed from the stainless steel but the x-rays "reflected" from the black deposit which was thick enough to prevent

[1] Blum and Hogaboom, *Principles of Electroplating and Electroforming*, 2nd ed., p. 276, 1930.

[2] Pfanhauser, *Galvanotechnik*, 7th ed., p. 432, 1928.

[3] Kersten, Rev. Sci. Inst. **3**, 145 (1932).

[4] Kersten, Rev. Sci. Inst. **3**, 384 (1932).

the lines due to the stainless steel from appearing on the film. The diffuse band indicates an amorphous structure.

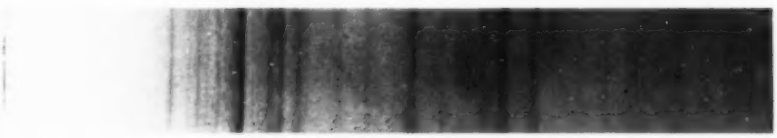

Fig. 2. Diffraction photograph of black nickel after it had been heated.

Fig. 2 shows the diffraction photograph of the same sample after it had been heated to redness in a covered procelain crucible over a Bunsen burner. The heating appeared to have driven off some of the sulphur. Some of the lines in Fig. 2 nearly correspond to those in the diffraction photograph of nickel, shown in Fig. 3.

Fig. 3. Diffraction photograph of nickel.

Fig. 4. Diffraction photograph of amorphous nickel sulphide.

Fig. 4 shows a diffraction photograph of nickel sulphide prepared by adding sodium sulphide to a solution of nickel chloride. It is evident that it is also amorphous but that there are two diffuse bands, neither of which corresponds to the one in Fig. 1, for black nickel.

An analysis of the black nickel, dried in a desiccator, showed that it contained 65 percent Ni, 10 percent S, 25 percent Zn. The same sample, after it had been heated to redness, contained 68 percent Ni, 7 percent S, and 24 percent Zn.

Capillary Flow Through an Ideal Uniform Soil

By W. O. SMITH
Pittsburgh, Pennsylvania

(Received June 25, 1932)

An ideal soil is an assemblage of spheres packed to a definite porosity, and for statistical purposes may be represented by grains placed in hexagonal array, with adjacent grain centers equidistant and at a distance $(2r+d)$, where r is the grain radius and d a spacing constant adjusted to suit the observed porosity. Three sets of capillaries, found to extend continuously throughout the packing, furnish the channels through which fluid crosses the soil body. The velocity through the mean capillary is calculated by a method essentially due to Slichter; and from this quantity, the sectional area of the mean capillary, and the number of capillaries per cm², the quantity of fluid per sec., f, crossing a soil of section area s and length L, is found to be

$$f = 0.00809\ (1-P)^{2/3}\{0.9850/(1-P)^{2/3} - 1\}^2\ \Delta p D^2 s/\eta L$$

P is the porosity, D the diameter of the grains, η the viscosity of the fluid, and Δp the pressure difference under which the flow occurs. Intrinsic permeabilities computed from this equation are compared with values for carefully sized glass spheres and quartz sands observed experimentally by Green and Ampt. A further comparison with corresponding values calculated from Slichter's equation is given.

AN IDEAL soil is an assemblage of spheres packed to a definite porosity; if the spheres are of one size, the soil is uniform. Corresponding respectively to the close and open packings of spheres in regular array, porosities are supposed to range from 0.26 to 0.48. Geometrically the assemblage may be regarded as generated by the distortion and warping of a regular lattice, and presents a system of elementary pore cells, such as that formed by three adjacent grains, and all of various sizes and configurations. Groups of these units, in turn, are found to be piled so that their interiors form a continuous tube extending across the soil body. Thus the whole assemblage is interwoven with a complicated net of capillary tubes running continuously throughout its extent, and these serve for the transmission of fluids across its interior.

While it is not possible to know the amount of fluid transmitted by each single capillary, the quantity crossing the soil each second may nevertheless be ascertained if the number of capillaries and the transmission of the mean capillary are known; and for this purpose the average packing must be considered.

For statistical purposes[1] the grains of the assemblage, still within the original confinements, may be regarded as moved into hexagonal array with adjacent grain centers equidistant, and at a distance $(2r+d)$; r is the grain radius and d a spacing constant adjusted to fit the observed porosity P. The quantity $(2r+d)$ is easily calculated; the number of spheres per cm³ is $2^{1/2}/(2r+d)^3$; this quantity multiplied by $4\pi r^3/3$ is the total sphere volume; hence

[1] Smith, Foote and Busang, Physics **1**, 18–26 (1931).

equating the latter to the total sphere volume $(1-P)$, expressed in terms of porosity, one finds

$$(2r + d)^3 = 4(2^{1/2})\pi r^3/3(1 - P). \quad (1)$$

When the grains of the assemblage have been so placed, there appear three sets of continuous capillaries extending through the packing; each of the planes (100), (010), (001), is traversed by a single set. The unit cell, that is the simplest element which when repeated yields the whole packing, is a rhombohedron of side $(2r+d)$ and face angles 60° and 120°. It is shown in Fig. 1, together with the three sets of capillaries, two piercing each face. The triangular tubes A and A' run approximately parallel to the edge bc; B and B' run parallel to ad; while C and C' run parallel to ab. The system is identical with that used by Slichter[2] for close packing of porosity 0.26; the unit cell, of course, is no longer of edge $2r$, but otherwise presents the same configuration. Each corner of the unit rhombohedron coincides with a grain center. The eight spheres, whose centers define the unit cell are shown in Fig. 2, together with two single capillaries AB and $A'B'$.

The course of a single channel is easily followed, for example $A'B'$ in Fig. 2 is observed to pass from the three-grain element composed of the spheres

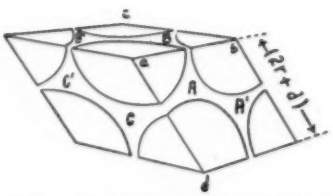

Fig. 1. Unit cell of edge $(2r+d)$ for spaced hexagonal packing.

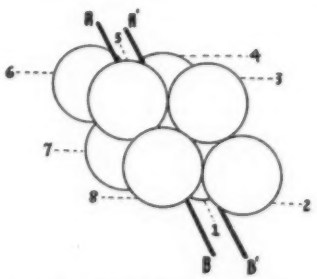

Fig. 2. Unit element of eight spheres.

1, 2, 8 in the $(00\bar{1})$ plane through the pore cell 1, 3, 8 in the (111) plane and out through the cell 3, 4, 5 in the (001) plane; hence each single capillary can be regarded as a chain of three grain pores. Fig. 3 is taken from Slichter's[2] work and presents the interior of the unit cell for close packing of porosity 0.26. The corners of the cell represent the centers of the grains shown in Fig. 2, and are numbered correspondingly. The concave spherical triangles such as abc are minimum pore sections, and three such are encountered by any capillary, such as $A'B'$, crossing the cell. The section of the capillary is thus cyclic, entering the cell at a minimum, expanding and again contracting to a minimum, and after another repetition leaving at a third minimum.

For any given position in the three-grain pore, the section of the capillary is approximately an equilateral triangle. While the grains are not in contact, save for close packing, the relative separation, as measured by the ratio of the separation d to the grain diameter D, is small. Even for the extreme case of 0.48 porosity the value of d/D is only 0.12. Fig. 4 shows a scale drawing for this case. The triangle a, b, c is equilateral and of the same area as the pore

cell bounded by the grains and relevant portions of the center triangle A, B, C.

Slichter[2] regarded the actual conducting capillary as having the section of an equilateral triangle, and calculated and mean fluid velocity from its average area and length. He assumed its section to be less than that of the pore, and considered it to be intermediate between the triangle inscribed in the pore and the pore itself. He then showed that although the velocity of flow through a tube of variable section was less than that through a tube having a uniform section equal to the mean section of the first tube because of the viscosity of the expanding and contracting stream, the velocity of flow through the second tube of mean section was not materially different, and not subject to any serious correction for the cyclic variation of the pore; hence the actual capillary could be replaced by one of mean section. The justification for considering the pore triangular, at least for the purpose of the flow problem, rests on the work of Boussinesq[3] who showed, for a number of shapes, that small changes in the form of cross section of a capillary do not appreciably alter the average velocity $\overline{U}$ across the section, provided the area is kept

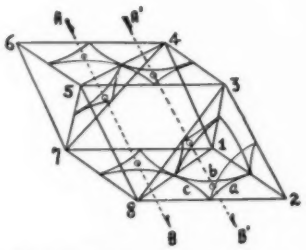

Fig. 3. Diagram showing the course of the conducting capillary through the cell.

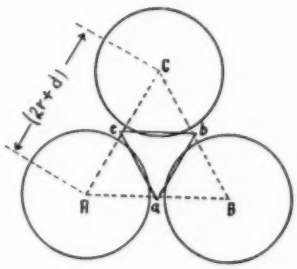

Fig. 4. Scale drawing showing minimum pore section of three-grain element for 0.48 porosity; the area of the equilateral triangle a, b, c equals that of the pore.

constant. The flow through an ellipse, for example, with semi-axes in the ratio 8/7 is only 1 percent less than that through a circle of the same area, and for the ratio 4/3 only 4 percent less.

The shape and configuration of the capillaries in the hexagonal array is the same as that used by Slichter for close packing; hence, in finding the velocity through the mean capillary, his work can be followed closely. The conducting capillary will be considered an equilateral triangle of uniform section equal to the mean pore section, and its area and length obtained by a method following closely that of Slichter. The justification for considering the section as an equilateral triangle, while subject to further investigation, will be considered as approximately established by the work of Boussinesq.[3] It is supposed, of course, that the separation of the grains is not sufficient to

[2] Slichter, 19 Annual Report U. S. G. S. Pt. **2**, 295–384 (1897–1898).

[3] Boussinesq, Jour. de Math. (2) **13**, 388 (1868); cf. Lamb, *Hydrodynamics* 5th ed., p. 556.

introduce serious error; cf. Fig. 4. Calculation will show the cyclic variation of the pore section to be of even less importance in its effect on the flow; Slichter's considerations were for an extreme case.

The area A of any section of the three-grain pore (cf. Fig. 4) is the area of the triangle through centers, $3^{1/2}(2r+d)^2/4$, less the area of portions of grains included, $(r^2-y^2)\pi/2$, where y is the distance between the given section and the plane of centers; hence

$$A = 3^{1/2}(2r + d)^2/4 - \pi(r^2 - y^2)/2.$$

The average area is given by

$$\bar{A} = (2/r)\int_0^{r/2} A\,dy = 3^{1/2}(2r + d)^2/4 - 11\pi r^2/24 \tag{2}$$

or from Eq. (1)

$$\bar{A} = 0.360D^2\{0.9850/(1 - P)^{2/3} - 1\} \tag{3}$$

where D is the grain diameter. In computing the average area it is to be noted that the centers of the grains of two adjacent pores of the capillary form a tetrahedron with the center of the common grain as vertex; hence the integration is from the plane of centers to a section lying at a distance $r/2$ above this. (cf. Fig. 2).

The course of the pore, if considered straight is parallel to an edge of the unit cell, and the length of the mean capillary is given by $\bar{L} = (3/2)^{1/2}L$, where L is the height of the soil column. The course, however, of the actual capillary is sinuous and deviates from a straight line. In Fig. 5 the heavy line

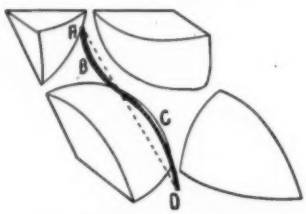

Fig. 5. The interior of the unit cell showing the curved axis of the triangular pore.

$ABCD$ marks the true course, while the dotted line represents the course considered as straight. Slichter[2] has shown that the length corrected for the curvature of the pore is 1.065 times $\bar{L}$; hence the true length L' of the capillary is given by

$$L' = 1.065(3/2)^{1/2}L. \tag{4}$$

The mean velocity through a triangular capillary is given by[4] $\bar{U} = 0.02887\,A\Delta p/\eta L$, where A is the area of section, η the viscosity of the fluid flowing, and Δp the pressure drop across the length L causing the flow. Hence the mean velocity of the fluid flowing through the mean capillary of the soil is from Eqs. (3) and (4)

$$\bar{U} = 0.00797\{0.9850/(1 - P)^{2/3} - 1\}\Delta pD^2/\eta L. \tag{5}$$

[4] Cf. Slichter, reference 2 or P. Forchheimer, *Hydraulik*, 3rd ed.

The quantity of fluid moved per sec. through each capillary is $\overline{UA}$; the number of capillaries per cm² is $1/A'$, where A' is the area of the triangle through the centers of the grains of a pore (cf. Fig. 4); hence the flow f, i.e., the quantity of fluid moved per sec., through a section of the soil column of area s is given by $f=\overline{UA}s/A'$. Since $A'=3^{1/2}(2r+d)^2/4=0.3545D^2/(1-P)^{2/3}$, we find using Eqs. (3) and (5) that the quantity of fluid flowing per sec. through the soil column of length L and section s, is given by

$$f = 0.00809(1 - P)^{2/3}\{0.9850/(1 - P)^{2/3} - 1\}^2\Delta pD^2s/\eta L. \qquad (6)$$

Two other quantities must be considered, namely the permeability and the intrinsic permeability. The quantity of fluid per sec. crossing unit area under a head of water, at unit density, equal to the length of the soil column is called the permeability and is defined by $F=fl/hs$. The product ηF is called the intrinsic permeability; η is the viscosity of the fluid flowing through the soil, and F the permeability. Since $\Delta p=gh$, we have from Eq. (6) with $g=980$ cm/sec.² that the intrinsic permeability is

$$\eta F = 7.93(1 - P)^{2/3}\{0.9850/(1 - P)^{2/3} - 1\}^2D^2. \qquad (7)$$

It will be observed that the quantity $\eta F/D^2$ depends only on the porosity.

The procedure used in deriving Eq. (6), while fundamentally identical with that of Slichter,[2] differs in two respects. First, it is to be observed that Slichter ultimately replaced the triangular capillary of mean section by a circular one having an area equal to the minimum pore section. It is not generally possible to do this, and certainly not for spaced hexagonal packing, since, as can be seen from Eq. (3) and (10), the ratio of the areas of the average to minimum sections depends on the porosity. Second, the packing is different. As unit cell, Slichter used a rhombohedron of edge $2r$, and face angle adjusted to suit the porosity; the face varied from a square for the most open packing to a rhombus of face angles 60° and 120° for the closest; the pores were therefore unsymmetrical. The unit cell underlying Eq. (6) is still a rhombohedron, but with fixed face angles of 60° and 120°, while the edge is adjusted to fit the porsity; the pores are always symmetrical, as indicated by probability considerations, and closely equilateral triangles as far as the continuous capillaries are concerned. Slichter obtained the equation

$$f = \frac{D^2}{96}\,\frac{sB^2}{(1 - S)}\,\frac{\Delta p}{\eta L} \qquad (8)$$

where $B=(1-\text{cosec }\theta/4)$ and $(1-S)=(\pi/6)(1-\cos\theta)^{-1}(1+2\cos\theta)^{-1/2}$. θ satisfies the equation, $2\cos^3\theta-3\cos^2\theta+1-(\pi^2/36)(1-P)^{-2}=0$.

The intrinsic permeability corresponding to Eq. (8) is

$$\eta F = 10.2D^2B^2/(1 - S). \qquad (9)$$

The equations for the flow f and the intrinsic permeability ηF hold not only for incompressible liquids, but also for gases if the volume of the ga transmitted per sec. is measured at the mean pressure, i.e., mean of the press sures at the ends of the soil column. This follows from the work of O. E.

Meyer[5] who has shown that the law of flow through capillary tubes holds for gases if the volume is measured as above.

Green and Ampt[6] made a careful investigation of the flow of air and water through columns of small glass beads, ranging in size from 0.0250 cm to 0.0938 cm, also through columns of carefully graded sands ranging in size from 0.0186 cm to 0.0825 cm in diameter. They found that while Slichter's Eq. (8) fits the data for sands very well it gave values for the glass beads anywhere from 50 to 85 percent too small; and concluded that since the beads were closely spherical and the sands were not, Eq. (8) was not quite correct. In Fig. 6 their experimental values of $\eta F/D^2$ are plotted for corresponding values of the porosity P. Curve A represents $\eta F/D^2$ as a function of P for Eq. (7), while the dotted curve B is the same relation for Eq. (9). It will be observed that Eq. (7) fits the data for round glass beads as marked on

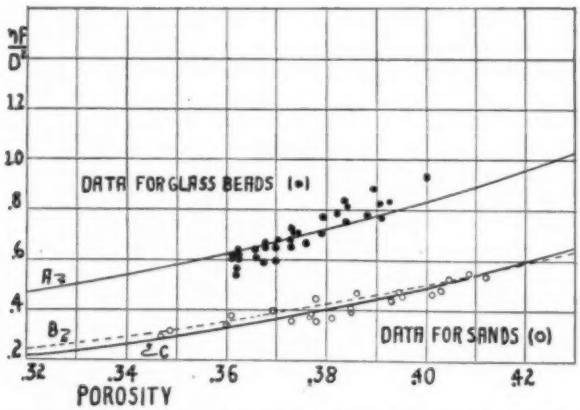

Fig. 6. The quantity $\eta F/D^2$ as a function of porosity; Curve A: Eq. (7); Curve B: Eq. (9); Curve C: Eq. (12); The data are that of Green and Ampt.

the figure, while the curve for Eq. (9), lying considerably below, agrees with the data for sands.

If, instead of the average section $\overline{A}$, the minimum pore section A'' is taken as that of the triangular capillary, i.e.,

$$A'' = 3^{1/2}(2r + d)^2/4 - \pi r^2/2 = 0.393D^2\{0.904/(1 - P)^{2/3} - 1\} \quad (10)$$

the flow through the packing, now regarded as occurring in capillaries of minimum section, is given by

$$f = 0.00965(1 - P)^{2/3}\{0.904/(1 - P)^{2/3} - 1\}^2\Delta pD^2s/\eta L \quad (11)$$

and ηF by

$$\eta F = 9.46(1 - P)^{2/3}\{0.904/(1 - P)^{2/3} - 1\}^2D^2. \quad (12)$$

The curve C of Fig. 6 represents $\eta F/D^2$ as a function of P for Eq. (12). This is observed to pass directly through the sand data. No particular stress,

[5] O. E. Meyer, Pogg. Ann. **127,** 269–270 (1866).

[6] Green and Ampt, Jour. of Agricultural Science **5,** No. 1, (1912–1913).

however, can be laid on Eq. (11), for in spite of the close agreement the assumption of a triangular capillary of minimum section has not been justified. I am unable, at present, to account for the close agreement except by attributing it to deviations of sand grains from sphericity.

TABLE I. *Summary of values of ηF and $\eta F/D^2$ for glass beads of various grades.*

Porosity P	Diameter of "beads" D	Intrinsic permeability $\eta F \times 10^3$				$\eta F/D^2 \times 10^3$		
		Observed by Green and Ampt		Calculated from Eq. (7)		Observed by Green and Ampt	Calculated from	
		Air	Water	Air	Water		Eq. (7)	Eq. (9)
0.391	0.0938 cm	6.76		6.88		768	782	464
.370		5.21		5.91		592	672	386
.3675		5.125		5.80		582	660	378
.3635		4.96		5.63		563	640	363
.3635			4.70		5.63	533	640	363
.400	.0709	4.685		4.20		931	835	500
.3925		4.19		3.97		833	790	470
.388		3.93		3.85		780	766	452
.384		3.806		3.74		756	745	435
.373		3.264		3.47		648	690	396
.373			3.33		3.47	663	690	396
.376	.0497	1.776		1.734		718	702	408
.373		1.677		1.704		677	690	396
.366		1.538		1.613		622	653	372
.366		1.564		1.613		634	653	372
.361		1.489		1.550		602	628	355
.361			1.523		1.550	615	628	355
.3895	.0319	0.901		0.790		885	775	460
.3835		.851		.756		835	742	435
.373		.736		.703		722	690	396
.3625		.626		.647		615	635	360
.3625			0.611		0.622	600	635	360
.384		.831		.759		815	745	436
.3795		.785		.734		771	720	420
.3745		.719		.704		706	695	402
.3705		.692		.688		679.5	675	388
.3705			0.6645		0.688	652	675	388
.382		.802		.749		787.5	735	425
.3735		.7195		.703		706.5	690	398
.368		.676		.674		663	662	380
.368			0.655		0.674	643	662	380
.3905	.0250	.516		.488		825	780	462
.384		.470		.466		752.5	745	436
.379		.4385		.450		702	720	419
.373		.4135		.433		662	690	396
.370		.4035		.420		645	672	386
.370		.410		.420		656	672	386
.366		.377		.408		603	653	372
.366			0.373		0.408	597	653	372

Table I shows the data of Green and Ampt for glass beads together with the values of ηF, and $\eta F/D^2$ for Eqs. (7) and (9). Table II shows the data and results for sands.

The problem of capillary flow in soils, as given above, differs from that of capillary rise reported in an earlier paper.[1] The packing employed here was used and good experimental agreement obtained. In that paper, however, the

TABLE II. *Summary of values of ηF and $\eta F/D^2$ for quartz sands of various grades.*

Porosity P	Diameter of "beads" D	Intrinsic permeability $\eta F \times 10^3$ Observed by Green and Ampt Air	Water	Calculated from Eq. (12) Air	Water	$\eta F/D^2 \times 10^3$ Observed by Green and Ampt	Calculated from Eq. (12)	Calculated from Eq. (9)
0.386	0.0825 cm	3.186		2.890		468	425	445
.378		3.018		2.655		443	390	414
.3695		2.706		2.450		397.5	360	383
.361		2.545		2.415		374	330	355
.3485		2.144		1.933		315.5	284	315
.347		2.070		1.905		304	280	310
.347			2.026		1.905	297	280	310
.412	0.0289	0.477		0.4590		535	550	550
.393		.3640		.3822		436	458	472
.385		.3265		.3507		391	420	440
.381		.3065		.3356		367	402	425
.378		.2955		.3255		353.5	390	413
.408		.4525		.4410		542	528	535
.395		.383		.3880		458.5	465	480
.403		.4005		.4190		479.5	502	514
.385		.3385		.3508		405.5	420	440
.401		.3885		.4115		465	493	505
.373		.294		.3115		352.5	373	396
.373			0.294		0.3115	352.5	373	396
.435	0.0186	.252		.2334		730	675	660
.4045		.1820		.1765		526.5	510	520
.3945		.1650		.1608		478	465	478
.377		.1320		.1332		382	385	410
.377			0.1290		0.1332	374	385	410

effective area and perimeter used to calculate the height of rise was a weighted mean, in which each of the pore sections occurring in the unit cell was weighted according to its frequency of occurrence. These can easily be identified in Fig. 2, and are the rhombus formed by grains 1, 2, 7, 8, the square formed by 3, 4, 7, 8, and the triangle formed by 1, 3, 8. For the purpose of this paper only one type of cell has been used, namely the triangular pore associated with the continuous capillary. The capillary rise problem involves either the filling or draining of pores; for equilibrium it depends only on the perimeter and area of the pore cells present in the meniscus, and it seems reasonable to suppose that all types of cells will be involved since all share in the filling or draining of the soil. In the flow problem, however, only the capillaries which exist continuously throughout the packing are capable of transmitting fluid after the assemblage is initially filled and steady flow takes place.

The Penetration of Hydrogen Through Steel at Four Thousand Atmospheres

By THOS. C. POULTER AND LESTER UFFELMAN
Department of Physics, Iowa Wesleyan College

(Received July 14, 1932)

A study is made of the penetration of hydrogen through a very fine grained steel as compared to the usual grade of steel used in the construction of pressure equipment. The penetration is studied in specially constructed cylinders and found to take place at much lower pressure than had previously been recorded. The penetrating effect of hydrogen is observed at as low as 4000 atmospheres, whereas 9000 atmospheres is the lowest pressure previously recorded for this effect.

PROCEDURE AND RESULTS

MANY investigators in studying high-pressure phenomena have found that certain liquids and gases may penetrate the walls of steel containers and greatly reduce their tensile strength. Perhaps the most notable of these are mercury and hydrogen,[1] although there is considerable evidence that a number of the more mobile liquids and several gases behave in similar manner but much slower. Not only is the tensile strength greatly reduced, but the crystalline structure is greatly modified. The fine granular structure is changed to a coarse structure resembling somewhat that of wrought iron. The hydrogen may be present as a pure gas, as a component of a mixture of gases, or in solution in a liquid.

It is usually impossible to find the openings in the cylinder walls even with a microscope unless the treatment with hydrogen is repeated several times. It occurred to the authors that it might be interesting to construct a cylinder out of two pieces of steel, one pressed inside of the other in such a way that after the hydrogen had penetrated the inner cylinder it might escape and not penetrate the outer cylinder. If the inner cylinder had a relatively thin wall, say 1/8 inch, the outer cylinder could then be made with such dimensions as to permit it to withstand a rather high pressure. Such a cylinder was constructed having an inside diameter of 1/2 inch and an outside diameter of 2 inches. The outside diameter of the liner was 3/4 inch giving it a wall thickness of 1/8 inch. On the outside of the liner and on the inside of the outer shell had been cut a very narrow and shallow groove or thread, through which the hydrogen, that had penetrated the inner liner, might escape.

The cylinder thus constructed was tested at 20,000 atmospheres, oil pressure. Hydrogen was generated in the cylinder by means of zinc dust and sulphuric acid and the pressure was transmitted by oil. The joint at the end of the cylinder, between the inner and outer shells was covered with a layer of oil so as to detect the escaping hydrogen. A pressure of 4000 atmospheres

[1] P. W. Bridgman, Rec. Trav. **42**, 568–71 (1923); Proc. Amer. Acad. Art Science **59**, 173–211 (1924).

was developed and allowed to stand for five minutes. At the end of this time a rapid evolution of hydrogen was noticed, followed shortly by the escape of a small quantity of the acid solution.

The cylinder was then washed and filled with oil, a pressure of 4000 atmospheres was developed and within five minutes a few cubic centimeters of oil had been forced through the pores produced by the hydrogen. The pressure was allowed to decrease as the oil passed through the inner cylinder walls, requiring two hours to reduce the pressure to 500 atmospheres. The pressure remained at 500 atmospheres for approximately one hour at which time the cylinder was removed from the press.

The inner liner was then removed and examined for flaws, but none could be detected even with a low power microscope. The liner was then immersed in water and filled with hydrogen at 100 pounds pressure. No bubbles were observed for approximately a minute, at which time the surface seemed to have adhering to it with a large number of very small bubbles which were difficult to see without the aid of a low powered microscope.

A similar assembly was constructed but having a liner made of a very fine grained high-speed steel. Since this steel is extremely brittle when heat treated it was machined from a piece of annealed steel and not further treated. In this case, a pressure of 4000 atmospheres was developed and allowed to remain for 20 minutes without any evidence of the penetration of hydrogen through the liner. The pressure was then built up to 6000 atmospheres at which pressure the hydrogen immediately penetrated. After allowing the hydrogen to pass through the liner for approximately one minute the pressure was released and the cylinder was cleaned out and filled with oil. A pressure of 8000 atmospheres was developed; allowed to remain for a few minutes with no indication that any oil had passed through the liner.

A Semiportable Alternating-Current Susceptibility Meter*

By WILLIAM M. BARRET**
Shreveport, Louisiana

(Received May 11, 1932)

This paper describes a semiportable alternating-current instrument that has been developed recently for measuring the magnetic susceptibility of geological samples. Its construction, basic theory, and operation are outlined briefly.

INTRODUCTION

EVERY recognized geophysical method depends for its operation on the nonhomogeneous character of the lithosphere. The various rocks that compose this outer shell of the earth exhibit differences in elasticity, density, electrical conductivity, and magnetic susceptibility. These variations give rise to the seismic, gravimetric, electric, and magnetic methods, respectively.

An intelligent interpretation of the anomalies related to these various methods must therefore be predicated on an intimate knowledge of the requisite physical constants of the involved media.

Numerous laboratory methods have been suggested for determining the magnetic susceptibility[1] of geological samples, though unfortunately, these methods have usually proved ill-suited to the requirements of the practicing geomagnetician. During the past year there has been developed in the laboratory of William M. Barret, Inc., an instrument that offers marked advantages from the standpoint of portability, rapidity of operation, ease of manipulation, and increased sentitivity and precision. This instrument, which has been designated an alternating-current *Susceptimeter*, is self-contained and portable, except for the fact that external power sources are required for its operation. It is the purpose of this paper to present briefly the essential characteristics of this instrument.

DESCRIPTION

The Susceptimeter, Fig. 1, consists primarily of a modified form of inductance bridge,[2] and an alternating-current galvanometer to indicate the condition of balance. The bridge is energized with 60-cycle, 110-volt alternating current, and in order to have no current flowing through the galvanometer the four arms of the bridge must be balanced for capacitance, inductance, and resistance. When these three elements are correct, the bridge is balanced and the galvanometer is at rest. Now, if in one arm of the bridge we insert a sample, whose susceptibility differs from that of air, into an appropriate test

* Read before the American Association of Petroleum Geologists at the Oklahoma City meeting, March 25, 1932, and printed in *Physics* by permission of the A. A. P. G.

** Geophysicist, William M. Barret, Inc., Giddens-Lane Building.

[1] Throughout this paper the term "susceptibility" will refer to volume-susceptibility.

[2] For a detailed discussion of a.c. bridge methods the reader is referred to B. Hague, *Alternating-Current Bridge Methods* (Sir Isaac Pitman & Sons, Ltd., New York).

coil, the balance is disturbed because the inductance of the test coil has changed. The balance is restored by altering the inductance of a variable inductor placed in the arm with the test coil. When this operation is completed, the reading of the inductor dial indicates, by means of a calibration curve, the susceptibility of the sample. These variations in inductance are frequently so very slight that the effect must be amplified by vacuum-tubes, and even then only the most sensitive galvanometers will prove suitable.

Electric Circuits

The electric circuits of the Susceptimeter are shown in Fig. 2. The ratio arms, R_1 and R_2, consist of equal pure resistances, while one inductive arm includes the test coil L_1 and variable inductor L_2, and the other contains the

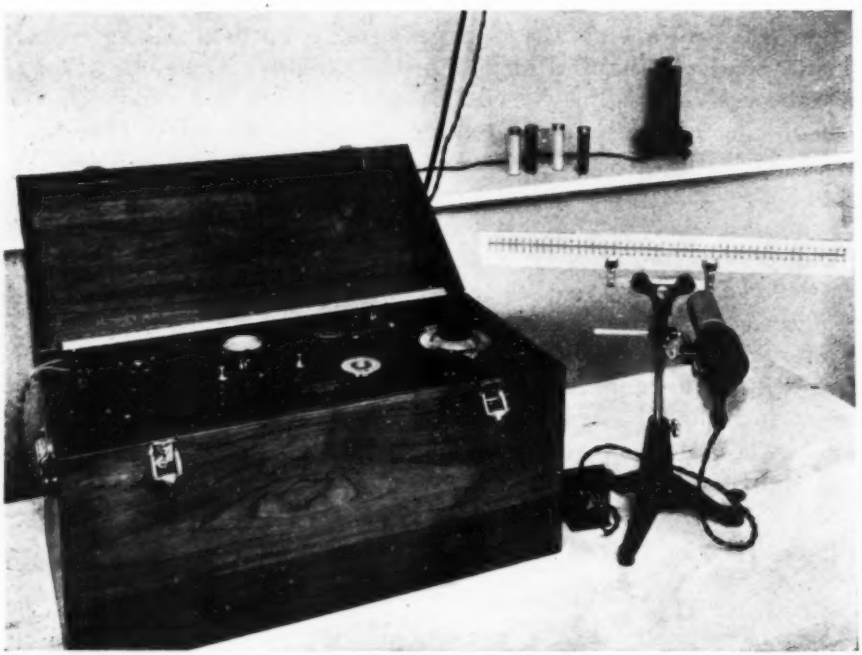

Fig. 1. Susceptimeter arranged for use with external vibration galvanometer. Several sample containers, filled with pulverized materials, may be seen near the galvanometer. These glass containers are provided with aluminum friction caps, and have outside dimensions of 2.7 cm dia. by 10 cm long.

tapped inductance L_3, and vernier variable inductor L_4. The resistance balance of the bridge is accomplished by means of r_5, and this balance is maintained for different positions of the inductance switch, S_1, by the loading resistors r_1 and r_2.

Low potential alternating current is supplied the bridge through the transformer T. The selector switch, S_4, and variable resistor, r_4, provide means for adjusting the bridge current, while its value may be determined with the ammeter A.

The indicating device consists of a pointer type, alternating-current galvanometer, energized by a three-stage, resistance-capacitance-coupled, vacuum-tube amplifier, which is provided with an appropriate output circuit that is designed to prevent the flow of direct current through the galvanometer circuit. The shunt r_3 permits critical damping of the galvanometer, and also furnishes a convenient means for adjusting its sensitivity. An external storage battery, B_1, supplies filament power for the amplifier, while the grid-bias battery, B_2, and plate battery, B_3, are included within the instrument case.

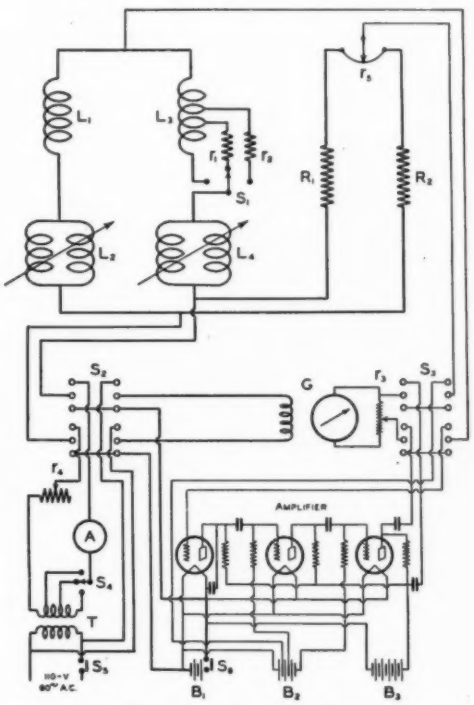

Fig. 2. Electric circuits of the Susceptimeter.

The switch S_2 makes it possible to energize simultaneously the bridge and galvanometer field winding with 60-cycle alternating current, or 6-volt direct current, while S_3 is for the purpose of connecting the galvanometer directly to the output junctions of the bridge, or including the amplifier in the indicator circuit. The switches S_5 and S_6 control the external alternating-current and direct-current power sources, respectively.

Theory

Let R_1 and R_2 be the resistances of the ratio arms; R_3 the resistance of the arm containing the inductances L_1 and L_2; R_4 the resistance of the arm containing the inductances L_3 and L_4; then, the condition imposed for a balance with direct current is $R_1R_3 = R_2R_4$ and by varying r_5 a balance can be obtained for steady currents.

When excited with sinusoidal currents, the general equation for balance with the inductance bridge is $LR_2 = L'R_1$, where L is the effective inductance of the arm containing L_1 and L_2, and L' is the effective inductance of the arm containing L_3 and L_4. The inductive balance is obtained by a proper adjustment of the vernier inductor L_4.

To avoid uncertainties occasioned by possible changes in the value of R_1 or R_2, the Susceptimeter circuit is based on the substitution method. When a sample, having a susceptibility differing from that of air, is placed in the test coil L_1, the inductance of this coil is changed, and to rebalance the bridge it is only necessary to alter the inductance of L_2, which is included in the arm with the test coil, by a like amount.

It is now required to express the relation between the susceptibility of the sample and the change in inductance of L_1 caused by its insertion. With no sample

$$N\phi = L_1 I \tag{1}$$

where N is the number of effective turns on L_1; ϕ is the total flux threading N effective turns; L_1 is the inductance of the test coil in c.g.s. units; I is the current through the test coil in c.g.s. units. Then, with sample inserted,

$$N(\phi + \Delta\phi) = I(L_1 + \Delta L_1) \tag{2}$$

and dividing (2) by (1)

$$\Delta\phi/\phi = \Delta L_1/L_1. \tag{3}$$

Also, with no sample present

$$\phi = A_s H_s + A_a H_a \tag{4}$$

where A_s is the cross-sectional area in cm² of the sample; A_a is the cross-sectional area in cm² of the annular space between the sample area and the mean area of the test coil; H_s is the effective magnetizing force in gilberts per cm in the sample; H_a is the effective magnetizing force in gilberts per cm in the annular space. When a sample of permeability μ_s is introduced into the test coil

$$\phi + \Delta\phi = \mu_s A_s H_s + A_a H_a \tag{5}$$

and subtracting (4) from (5) $\Delta\phi = A_s H_s(\mu_s - 1)$.

Expressing μ_s in terms of the susceptibility, κ_s, we may write $\Delta\phi = A_s H_s \cdot 4\pi\kappa_s$. Substituting this value of $\Delta\phi$ in Eq. (3) and solving for κ_s, we have

$$\kappa_s = \Delta L_1 \phi/(A_s H_s \cdot 4\pi L_1) = C \cdot \Delta L_1 \tag{6}$$

where C is a constant for the fixed frequency, and for the current range available.

In Eq. (6), ΔL_1 is determined by means of the variable inductor L_2; the product $A_s H_s$ is measured with a search coil and ballistic galvanometer; L_1 is measured in place with an external inductance bridge, and ϕ is calculated from flux measurements made through various sections of the test coil.

Operation

In operation, the Susceptimeter circuits are first energized with direct current, and a resistance balance obtained by varying r_5. Following this, the

bridge is excited with alternating current, and the galvanometer and amplifier connected in the indicator circuit. With no sample in the test coil L_1, and with the variable inductor L_2 adjusted for maximum inductance (dial reading 0), the vernier inductor L_4 is used to bring the galvanometer pointer to mid-scale position.

If a specimen, having a susceptibility greater than air, be now introduced into the test coil, the galvanometer pointer will move toward the positive side of its scale, and to rebalance the bridge it will be necessary to reduce the inductance of L_2. This is accomplished through the aid of a micrometer drive mechanism, provided with a vernier dial, which makes it possible to adjust and read the position of the variable inductor to within 1/100 scale division. The proper decrease in L_2 is obtained when the galvanometer pointer again

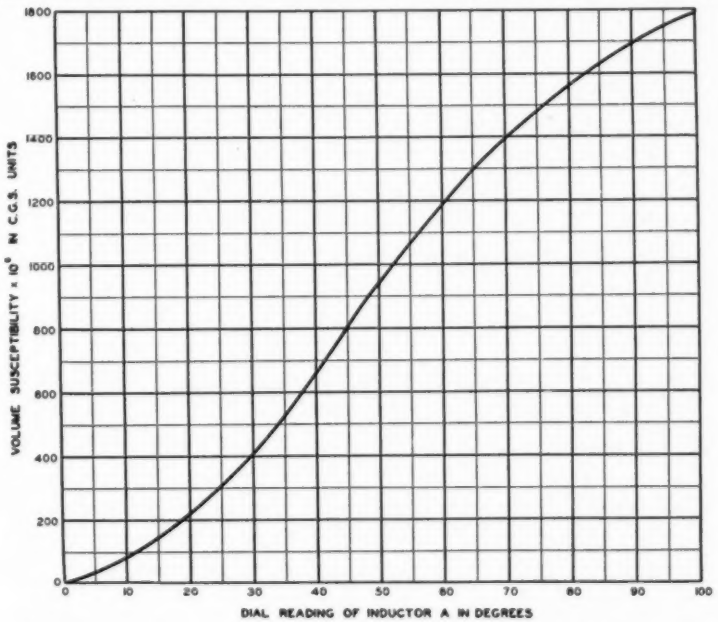

Fig. 3. Normal calibration curve for first selector switch position. For second or third position, a constant additive correction is applied, its value depending on switch position used.

assumes its equilibrium position. The dial reading of the variable inductor is then a measure of the susceptibility of the unknown sample, and by employing a calibration curve similar to Fig. 3, the dial readings may be conveniently converted to susceptibility values. To extend the range of the instrument, the tapped inductance L_3, and selector switch S_1 are used. When the second or third selector switch position is required, a constant additive correction is applied to the normal calibration curve, the value of the correction depending on the switch position used.

Should a diamagnetic specimen be inserted in the test coil, the galvanometer pointer moves in the direction of the negative part of its scale, and for this condition, the initial balance is obtained with the inductor L_2 set at some arbitrary scale position, and then its inductance increased until the galvanometer again indicates a balance. The same calibration curve employed

for paramagnetic materials will serve for diamagnetic substances, simply by noting the initial and final scale positions of L_2 and reading the respective difference, in terms of κ, from the curve.

General

For convenience, the samples are used in the pulverized state, and when carefully prepared their density seldom differs markedly from that of the original material. Belz[3] and Wilson[4] have found that equal masses of several paramagnetic substances have the same magnetic susceptibility in the solid as in the powdered form.

The susceptibility is a function of the effective magnetizing force[5] for many materials, and for this reason it is well to use a fixed value of field strength for comparative studies. Within narrow limits, the magnetizing force applied to the sample is directly proportional to the bridge current.

As most electrical methods for measuring the susceptibilities of rocks have employed direct current, the question naturally arises as to the authenticity of determinations conducted with alternating current. Two possible sources of error are at once apparent, i.e., those caused by virtue of the specific inductive capacity of the sample, and its electrical conductivity. In order to determine the influence of the dielectric constant, a specimen of distilled water was examined. While this specimen exhibited a high dielectric constant and low conductivity, no observable effect was noticed. Also, it was found that a saturated solution of sodium chloride, having a high conductivity, failed to produce a sensible deflection of the indicator, which is in agreement with the similar investigations of Rücker.[6] As the values of dielectric constant and conductivity of these samples are much higher than those customarily encountered in practice, it is felt that these factors may be safely ignored.

The susceptibilities of ferromagnetic substances are extremely high for very low frequencies, and unity for all materials in the magnetic fields of light and infrared waves.[7] However, Brown[8] has shown that the susceptibility of iron in oscillating magnetic fields of less than 300,000 cycles per second is approximately constant and similar to that in stationary fields.

While variations in κ occur over tremendous changes in frequency, nevertheless, for routine measurements with geological specimens, where the numerical values of susceptibility, dielectric constant and conductivity are usually low, the discrepancy introduced by using 60-cycle current is negligible. In fact two important technical advantages result from the application of alternating current, (1) freedom from extraneous magnetic disturbances that react unfavorably on many direct-current and magnetometric methods, and (2) the susceptibility measurements are independent of the previous magnetic history of the sample.

[3] M. Belz, Phil. Mag. [6] **44,** 479–501 (1922).

[4] E. Wilson, Proc. Roy. Soc. **A96,** 429 (1919).

[5] P. Weiss, *Recherches sur l'aimantation de la magnétite cristallisée.* L'Éclairage Électrique **7,** 487 (1896).

[6] A. W. Rücker, Proc. Roy. Soc. London **48,** 515 (1891).

[7] W. Arkadiew, Phil. Mag. [6] **50,** 157–163 (1925).

[8] R. Brown, Jour. Frank. Inst. **183,** 41 (1917).

Reduced Scale Studies in Armor Penetration

By L. THOMPSON
Naval Proving Ground, Dahlgren, Virginia

(Received April 18, 1932)

The attack of armor by competent projectiles involves a punching cycle of very short duration and extreme reactions. The characteristic results, with respect to the essential properties in the design of ship protection, have been investigated by means of simple dimensional forms, and a generalization has been made by reference to a penetration coefficient. The latter is a function of the penetration number (ratio of plate thickness to projectile diameter) and the obliquity of impact. A similar treatment of the absorption problem is outlined, and the special case of thin plate is of note in the implied linear velocity law of reaction. Conditions for extension in scale are stated and also certain convenient ratios for the estimation of the relative limits of nonsimilar systems.

THERE are two classes of plate penetration data which are of practical importance. The first concerns the so-called "limits" of a structure. A limit velocity is just sufficient to produce complete penetration of the plate or structure at a given angle of attack by the projectile of size and design under consideration. That is, the projectile has a velocity such that its energy is just enough to punch a hole and pass through to a position behind the plate. The angle of obliquity is measured from the normal to the plate surface and the limit velocity increases, of course, as the obliquity is increased. The second class of data is concerned with absorption. It is often desirable to predict the velocity or energy remaining after a complete penetration, the striking velocity being above the limit. Both sets of data are of use in the design of armor protection for ships, and it is of advantage to have a general empirical basis for the prediction of full-scale results without the requirement of extensive calibration tests for each condition.

Velocity Limit Correlations

Assuming that the normal component of the striking velocity V_2 required just to penetrate a plate (of a specific kind) of thickness e, with a projectile of diameter d at obliquity θ, is defined by the variables $V_2 \cos\theta \equiv V_n(M, \theta, e, d, T_0)$, M, mass projectile; T_0, factor in plate constant, having dimensions of energy; V_n, velocity component normal to plate; k, constant, it has been shown by dimensional conditions,[1,2] that

$$V_2 = k(e^{1/2}d/M^{1/2}\cos\theta)F(e/d, \theta). \tag{1}$$

The function $F(e/d, \theta)$ is then the penetration coefficient, being an index of quality of performance either of the plate or of the projectile depending on which is being proved, and its satisfactory identification provides the desired

[1] L. Thompson, U. S. Naval Inst. Proc. **56**, 5 (1930).
[2] L. Thompson and E. B. Scott, Memor. del'artill. Franc. **6**, 4 (1927).

facility for the prediction of the velocity limits of armor plate systems. The ratio e/d may be called the penetration "number," having a significance analogous to that of the ratio velocity/velocity of sound, or of Reynold's number, in respect to the resistance function of hydrodynamics.

All of the results obtained in the measurement of plate-limit velocities (determined by obtaining a "straddle," that is, a velocity just above and just below the limit) with projectiles from 4 to 16 inches in diameter and with plates (of one class) of the various thicknesses of service application, for obliquities from 0° (normal impact) to 30°–75°, the maximum obliquity depending on thickness, have been summarized by reference to this form.[3] The general nature of the coefficient function is shown in Fig. 1. It is linear in the variable e/d and the contours intersect at a value of e/d somewhat less than 0.5, in the vicinity of which the limit velocity therefore varies directly with the secant of the angle of obliquity.

For a particular class of projectiles and of plate, it has been well established that the type of representation is adequate throughout the range of interest. The probable deviation of the average of results for several plates, at

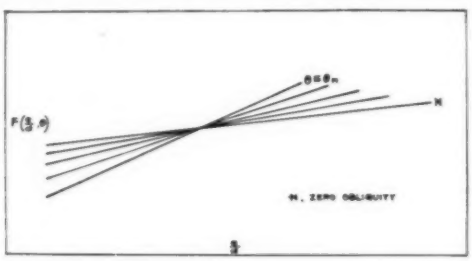

Fig. 1.

any point in the field, from the representative contours, is of a smaller order than the probable sampling variation from plate to plate. A continuously developed plot of experimental coefficients provides a convenient basis (as, for example, in the case of the model basin or wind tunnel) for interpreting the results of any specific proof test and at any practicable scale, in accordance with the standards of past experience for similar conditioning.

The limit summary has been stated, also, in the following form[4] to facilitate certain applications:

$$F = k_1(\theta^2 + a)(e/d - 0.45) + P,$$

k_1, a, P are constants; from which

$$V_2 = [k_2 e^{0.5}(e - 0.45d)(\theta^2 + a) + P_1 d]/M^{0.5} \cos\theta. \qquad (2)$$

[3] An application to (small arms) bullets has also been completed in collaboration with Lieut. Comdr. Leighton Wood, U. S. Navy.

[4] The empirical penetration formulas of de Marre, Krupp and Moisson may be compared:

de Marre	$V = Ce^{0.7} d^{0.75} M^{-0.5}$
Modified de Marre	$V = Ce^{0.7} d^{0.75} M^{-0.5} f_2(\theta)$
Krupp	$V = Ke^{0.5} d(e/d)^{1/6}/M^{0.5} \cos\theta$
Moisson	$V = K_1(de^2/M)^{1/3}$ (for $\theta = 0°$)

Referring to the conditioning of tests, similarity is evidently realized (for any one class of plate and of projectiles) where e/d and θ values are maintained; that is, for the same ratio of plate thickness to projectile diameter and the same obliquity. The following cases are of interest: (1) Two plates of different thicknesses will have the same limit velocity when attacked at the same obliquity by similar projectiles of diameter in the ratio $d_1/d_2 = e_1/e_2$. This follows from the definition 1 since

$$e^{1/2}d/M^{1/2} = (e/d)^{1/2} \cdot d^{3/2}/M^{1/2}$$

and $M = k'd^3$, (that is, the weights of similar projectiles are as the cubes of the diameters). (2) In general, limit velocities for similar projectiles are to each other as the square roots of the e/d ratios multiplied by the F ratios and secant θ ratios. Special cases include the following: Limit velocities are to each other, (a) if $d_1 = d_2$, directly as values of F sec θ and as the square roots of plate thickness. (b) if $e_1 = e_2$, directly as F sec θ and inversely as the square roots of projectile diameter. (c) if $\theta_1 = \theta_2$, directly as coefficients F and as the square roots of the scale variable e/d. (And if $(e/d)_1 = (e/d)_2$, $V_{L_1} = V_{L_2}$.)

Absorption Summary

The loss of energy ΔT in passing through an armor plate is assumed to be identified by the following variables:

$$\Delta T \equiv \Delta T(T_s, V_s, V_L, e, d, \theta)$$

T_s, V_s being striking energy and velocity, respectively. It is then obtained by usual procedure that

$$\Delta T = T_s f(e/d, V_L/V_S, \theta)$$

the scale variables being the penetration number, the ratio of striking velocity to limit velocity and the obliquity.

Data accumulated with major and minor caliber projectiles have established tentatively the following form:

$$\Delta T = T_s m(e/d, \theta)[V_L/V_S - (V_L/V_S)_0] + K(e/d, \theta). \qquad (3)$$

The characteristics of the factors $m(e/d, \theta)$, $(V_L/V_S)_0 \equiv f_a(\theta)$ and $K(e/d, \theta)$ have been made available in a suitable graphical representation.

Discussion

As a test of plate quality, it is evident that absorption data, if of comparable precision, can be utilized quite as well as actual limit determinations, with the advantage that definite test velocities can be used for all plates, depending on thickness and obliquity only, and with the economy of fewer rounds. The data obtained by firing one round then constitute a complete basis for identifying the quality of the element under test, insofar as the uniformity of material is not questioned.

The penetration of thin armor is a special case of interest. Thin plate is defined as armor of thickness small with respect to projectile diameter. As the impact develops, the plate area is deformed more or less uniformly, depend-

ing on the velocity of the projectile and obliquity of impact, with no definite "button" formation analogous to that of thick plate penetration. The button developed in the perforation of thick plate is often projected behind the plate as a "punching" of one or two large pieces.

It has been noted in prior discussions[2] that a resistance law linear in velocity would lead to a nearly constant velocity absorption with increasing striking velocity. Actual results define, in general, an increasing energy absorption, as expected, but a decreasing velocity loss as the impact velocity is increased. The absorption of energy increases too slowly with increase of striking velocity beyond the limit for the structure (or, it may be said, the velocity lost in the punching cycle decreases too rapidly) to permit the effectiveness of divided armor to equal that of solid plate; the limit formula and the absorption function characteristics together account for the observed properties of divided or laminated armor. The error is sometimes made of assuming a solid-plate limit penetration formula alone competent to establish the limit for a divided plate structure. For example, Rougeron[5] states that the reduced effectiveness is predicted by the specific empirical form given by de Marre. For thin plate, however, the velocity absorption may be actually constant over a wide range of velocities, particularly at the higher obliquities. In that case, the effective resistance is at least approximately proportional to the velocity. For the momentum-impulse equation can be written,

$$\Delta V = \frac{1}{M}\int \frac{F_1(v, s)ds}{v(s)}$$

$F_1(v, s)$ resistance function, s phase of penetration, M projectile mass, and, (since for thin plate $\Delta V(e, d, \theta)$ is taken to be constant for any distribution of velocities), it follows that $F_1(v, s)/v$ is a function of s only, that is $F_1/v \equiv f_1(s)$, or $F_1(v, s) \equiv v f_1(s)$.[6] Thus for these conditions the resistance function is evidently of the form

$$R = cv f_{11}[s/(e + 2d), \theta, \psi], \qquad f_{11} = 0 \text{ for } s = e + 2d \text{ or } 0$$

ψ ogival angle of the projectile (form variable), θ obliquity of impact, $c \equiv c(d, e)$, (the dissipative reaction is reduced to a small quantity when the penetration has reached a value equal to twice the diameter of the projectile plus the effective thickness of the plate).

Lieutenants K. M. McLaren, M. E. Murphy, F. S. Withington and L. E. Reinken, U. S. Navy, have made some recent adjustments of the plate coeficient function, evaluated the constants of the absorption summary and prepared a convenient set of nomograms covering the applications.

[5] C. Rougeron, La Revue Maritime, May 1931. (Translation, R. T. Hanson, U. S. Naval Inst. Proc. February, 1932.) In this connection it is of interest to note that E. Bianco di S. Secondo introduces a similar difficulty (Rivista Marittima, December, 1931) in assuming that the velocity remaining after penetrating a plate of thickness e, with impact velocity equal to the limit for a solid plate of thickness $(e+f)$, is equal to the limit for a plate of thickness f.

[6] I am indebted to Professor C. C. Bramble for criticism with respect to this statement.

THE EDITOR'S COLUMN

Atomic Disintegration by Artificially Accelerated Protons

EVEN those physicists who have been most closely familiar with research on the atomic nucleus, and who have felt for several years that they were on the verge of rapid expansion of their knowledge, are astonished at the sudden burst of fundamentally important new facts which have come to hand in the last twelve months. Some of these have already been discussed in previous issues. The newly discovered neutron was made the subject of an account in April and the interaction of cosmic rays and atomic nuclei was mentioned in May. It is at present correct to say that neutrons and cosmic rays are phenomena closely related to atomic nuclei. However, this may be the case only for the very penetrating cosmic rays and the very energetic neutrons to which our present knowledge is limited.

Within the last six months a new line of evidence bearing on nuclear structure and behavior has come to light and gained the keen interest of the world. It has come not by chance or accident but by intelligently directed research,—and has come sooner than was expected. It is the disintegration of atoms by the impact of fast moving protons. Scarcely a month passes now without newspaper headlines telling of another "atom smashing machine." This account will be confined to the first of these revolutionary experiments.

Most readers of this column are aware that atoms have been "smashed" at will in our laboratories for many years. They can also distinguish the temporary and self-repairing "smashed atoms," which are only smashed in their outer electronic structure, from the really and permanently smashed atoms whose nuclei have been disintegrated or built up. It is with operations on the nucleus itself that the alchemist must deal, and only now has he gained possession of adequate tools.

The development of these tools was given direction by the discovery that fast flying α-particles naturally given off in spontaneous radioactive transformations could occasionally eject, out of nuclei with which they collided, particles later identified as protons. This discovery was made by Lord Ernest Rutherford in 1919 and immediately it was realized that whenever men could produce fast α-particles by artificial means, at least some of the chemical elements could be converted into others at will. The energy possessed by α-particles is of the order of 4 to 8 million ϵ-volts, however, and at that time the most energetic moving charged particles produced in the laboratory were the cathode rays—fast electrons accelerated in evacuated vessels more or less like x-ray tubes. The energies available were of the order of 100,000 ϵ-volts.

The development which was then commenced—and is now being fruitful—soon resolved itself into the solving of two problems. First, it has been necessary to find ways of generating differences of potential of the order of millions of volts, and second, vacuum tubes had to be so designed that application of such high voltages did not produce their immediate destruction. A review of some of this development was given in these columns last November.

One laboratory where a particularly ambitious attack has been made on the problem of producing fast particles is the Cavendish Laboratory at Cambridge, England. Working under Lord Rutherford as Director of this Laboratory, J. D. Cockcroft and E. T. S. Walton[1] developed and successfully operated an apparatus which could produce fast protons having energies of several hundred thousand ϵ-volts. They found it more convenient to produce fast protons than artificial α-rays and were content with this because the concepts of the new quantum mechanics indicated that protons would be the more effective of the two in penetrating the atomic nucleus.

Their very first result was startling in the

[1] J. D. Cockcroft and E. T. S. Walton, Nature **129**, 649 (1932); Proc. Roy. Soc. **136**, 619; **137**, 229 (1932).

extreme, because they found that bombardment by protons of only 125,000 volts energy caused the disruption of lithium atomic nuclei. The value of the higher voltages at their disposal was immediately apparent, however, because they found that the yield of disintegrations per million striking protons was rapidly increased as the voltage was raised. At 125,000 volts they observed less than a hundred disintegrations per million protons.

It is necessary to make clear just what was observed because only in this way can the second startling result of the experiment be described. The protons were made to strike a thick foil of lithium metal which was mounted inside of the evacuated experimental tube. Opposite this foil, which was slanted as a house-roof is to the rain, were two thin mica windows in the wall of the tube, one exposed to the under, the other to the upper surface of the lithium foil. Outside these windows were placed glass plates coated with a crystalline material which shows a bright microscopic scintillation when it is struck by an α- or other fast moving particle. When protons were striking the lithium, observers with microscopes could see scintillations on these screens. The effect was stopped by removing the lithium or cutting off the impinging protons.

The scintillations were not produced by scattered or reflected protons because the mica windows were too thick to let them through. In fact, no particles capable of producing scintillations could have come through the windows without possessing very much more energy than the original protons. Here then is a second new result. The only possible interpretation is that the protons act like triggers and cause something like an explosion of the lithium nucleus struck. The energy released is greater than that furnished to release it.

By the use of other auxiliary apparatus the observations have been carried further. The ejected particles causing the scintillations turned out to be α-particles. By observation of both windows it has been found that they tend to appear in pairs suggesting that each lithium nucleus explosion gives rise to *two* fast α-particles. If this is the case then the data are available to write a reaction equation which may correctly describe the entire event:

$$Li^7 + p = 2\alpha + W.$$

This equation expressed the postulate that a nucleus of the second isotope (mass = 7) of lithium combines with the striking proton and yields two alpha-particles with an amount of kinetic energy equal to W. (It is generally believed that the Li^7 nucleus is composed of seven protons and four electrons. By adding the impinging proton the necessary eight protons and four electrons for the constitution of the two α-particles are obtained.) Evidently we here see the opening of a new chemistry, the chemistry of interacting atomic nuclei. It is quite conceivable that this is the only chemistry applicable in some parts of the universe, notably in the hot centers of the dense stars.

The crowning beauty of the above interpretation remains to be stated. The mass of the Li^7 atom is accurately known and so are those of the α-particle and of the proton. The masses in the equation do not precisely balance. That is, the two α-particles do not contain quite as much as the original reacting Li^7 and proton. The lost mass, when converted into energy units by the Einstein relativistic formula, should provide 15×10^6 ϵ-volts of energy. The preliminary experiments of Cockcroft and Walton[1] show, within a reasonable limit of accuracy, that the total kinetic energy of the two flying α-particles is just about this amount. If more accurate experiments confirm this result, then this early experiment in nuclear chemistry has an important quantitative as well as a qualitative significance, and it may be used to confirm the concept that matter can be changed into energy.

H. A. BARTON